CHEMICAL ENGINEERING TRANSACTIONS
VOL. 70, 2018
A publication of AIDIC
The Italian Association of Chemical Engineering
Online at www.aidic.it/cet
Guest Editors: Timothy G. Walmsley, Petar S. Varbanov, Rongxin Su, Jiří J. Klemeš

ISBN 978-88-95608-67-9; **ISSN** 2283-9216
DOI: 10.3303/CET1870128

The Ammonia Looping System for Mid-Temperature Thermochemical Energy Storage

Giuseppe Masci[a,c], Carlos Ortiz[b], Ricardo Chacartegui[c,*], Vittorio Verda[a], Jose M. Valverde[b]

[a]Department of Energy Engineering, Politecnico di Torino, Corso Duca degli Abruzzi 24, 10129 Torino, Italy
[b]Facultad de Física, Universidad de Sevilla, Avenida Reina Mercedes s/n, 41012 Sevilla, Spain
[c]Escuela Técnica Superior de Ingeniería, Universidad de Sevilla, Camino de los descubrimientos s/n, 41092 Sevilla, Spain
ricardoch@us.es

Thermochemical reactions have a great potential for energy storage and transport. Their application to solar energy is of utmost interest because the possibility of reaching high energy densities and seasonal storage capacity. In this work, thermochemical energy storage of Concentrated Solar Power (CSP) based on an ammonia looping (AL) system is analysed. The AL process for energy storage is based on the reversible reaction of ammonia to produce hydrogen and nitrogen. Concentrating solar energy is used to carry out the decomposition endothermic reaction at temperatures around 650 ºC, which fits in the range of currently commercial CSP plants with tower technology. The stored energy is released through the reverse exothermic reaction. Our work is focused on energy integration in the system modelled by pinch analysis to optimize the process performance and competitiveness. As result a novel configuration is derived which is able to recover high-temperature heat for electricity production with a thermal-to-electric efficiency up to 27 %. The current study shows a clear interest of the system from an energy integration perspective. Further research should be conducted to access the potential for commercial applications.

1. Introduction

Solar energy has a main role in a sustainable future mainly due to the huge amount of solar irradiation arriving to Earth. Concentrated solar power (CSP) is particularly attractive due to their dispatchability potential and scalability (Mehos et al., 2016). A promising technique to store and dispatch solar energy on a 24-h basis is Thermochemical Energy Storage systems (TCES) (Dunn et al., 2012). This paper is devoted to the energy integration analysis of the coupling of CSP with a TCES system based on the reversible reaction of ammonia - Eq(1), which is a widely used process in other industrial applications (Modak, 2011):

$$2\mathrm{NH_3} + \Delta\mathrm{Hr} \rightleftharpoons \mathrm{N_2} + 3\mathrm{H_2} \qquad \Delta\mathrm{Hr} = 66.8\ \mathrm{kJ/mol} \tag{1}$$

In this storage system, ammonia is cyclically passed between a solar dissociation reactor and a synthesis reactor, both containing a catalytic bed. The reaction mechanism of ammonia dissociation and synthesis has been widely studied and recently revisited in (Boisen et al., 2005). Previous works on TCES based on ammonia have proposed a decomposition temperature of 850 ºC (Kreetz and Lovegrove, 1999). According to (Luzzi et al., 1999), the expected net solar-to-electric conversion efficiency is about 18 % in a demonstration CSP system based on the parabolic dish solar collector technology whereas the net thermal-to-electric efficiency achieves values close to 30 %. A study on the transient performance of TCES ammonia cycle has been reported in (Abdiwe and Haider, 2017). (Kreetz et al., 2001) analysed the optimisation of the thermal output in the synthesis reactor, which introduced a novel configuration able to guarantee similar thermal-to-electric efficiency to that proposed in (Luzzi et al., 1999) by using a lower temperature source. In regard to catalysts used in ammonia reactions, a wide number of candidates have been analysed (Liu, 2014).

Please cite this article as: Masci G., Ortiz C., Chacartegui R., Verda V., Valverde J.M., 2018, The ammonia looping system for mid-temperature thermochemical energy storage , Chemical Engineering Transactions, 70, 763-768 DOI:10.3303/CET1870128

The goal of the present work is to evaluate the thermodynamic performance of a 100 MW_{th} concentrated solar power plant coupled with a novel ammonia looping configuration (CSP-AL) to provide electrical energy during a 24h base load operation plant. As main novelty, a reduction in the dissociation reactor temperature is proposed in order to increase the competitiveness of the technology by using a mid-temperature solar source (650 °C). This study aims at identifying the main thermal and exergy losses of the plant, as well as improving thermal integration and performance. The optimized integration has been performed via a detailed pinch analysis of both endothermic and exothermic sides. The obtained results for this integration are promising. Advantages and disadvantages in comparison with other potential TCES systems are highlighted.

2. The ammonia looping process model

The Ammonia Looping (AL) process starts with the decomposition of ammonia (Eq(1)). The reaction by-products exiting the dissociation reactor are used to preheat the ammonia stream and are cooled and separated afterwards. Unreacted liquid ammonia is recirculated into the solar reactor. The gaseous products (hydrogen and nitrogen) can be either stored or sent to a synthesis reactor for power production depending on the production pattern. The use of a split ensures flexibility with regarding electricity production. When energy is needed, the stored by-products are sent to another reactor where ammonia synthesis occurs.
The departure layout of the CSP-AL integration is shown in Figure 1. A heat exchanger (HX-A) is allocated between the dissociation reactor and the separator in order to improve heat integration at the endothermic side. The gaseous products (hydrogen and nitrogen) are separated in the separator from ammonia, which tends to liquefy spontaneously as the temperature decrease. Later on, the gas stream (H_2 and N_2) is compressed up to the exothermic reactor pressure. Two stages of compression with intercooling are considered wherein the intermediate pressure is calculated as the harmonic mean of the two extreme pressures.
Model simulations have been carried out by using Aspen Plus™. In the model (Lovegrove, 1996), a set point temperature of 650 °C and a pressure of 114 bar have been used for the dissociation reactor, which leads to an ammonia conversion of 0.6 (Lovegrove, 1996). High pressure ammonia synthesis experiments have been reported in (Kreetz and Lovegrove, 1999). Results on the reaction extent (or N_2 conversion) showed that, considering a pressure of 150 bar, the maximum conversion obtainable in the synthesis reactor was ~0.4 at a temperature of 450 °C. The heat released by the ammonia synthesis reaction is used for power production by means of a steam cycle working at 430 °C (20 °C temperature difference with the synthesis reaction temperature) and 100 bar as live steam conditions (Luzzi and Lovegrove, 1997).

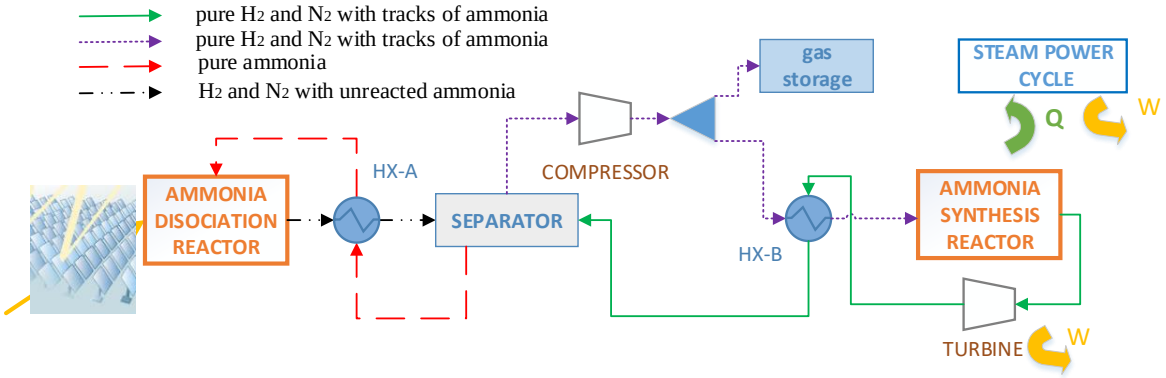

Figure 1: Flowsheet of Base Case, Layout 1

The following assumptions were considered for simulations: i) steady state analysis; ii) complete separation process (ammonia does not liquefy completely in the separator at any pressure); iii) kinetics of reactions do not depend on mass flow rate; iv) inlet solar thermal power is fixed to 100 MW during 8h/ d; v) in the charging phase, a 1/3 of the stream flows are sent directly to the power production side whereas the rest is sent to storage; vi) no pressure drops have been taken into account; vii) the minimum temperature approach for all heat exchangers has been kept constant and equal to 20 °C, and vii) in the separator, streams are cooled to the ambient temperature (20 °C). The thermal-to-electric efficiency has been estimated by Eq(2). Table 1 shows the main inputs and outputs from the base case simulation.

$$\eta_{el} = \frac{\text{net electric power produced [MWe] x 24 [h]}}{\text{net solar thermal power [MWt] x 8 [solar h]}} \quad (2)$$

Table 1: Main operation parameters of the plant.

Endothermic side		*Exothermic side*		*Others*	
specification	value	specification	value	specification	value
net solar thermal power	100 MW	net thermal power	46 MW	Storage pressure	150 bar
reaction pressure	114 bar	reaction temperature	450 ºC	Storage temperature	20 ºC
reaction temperature	650 ºC	reaction pressure	150 bar	Steam cycle pressure	100 bar
ammonia mass flow rate	30 kg/s	expected conversion of hydrogen	0.4	Steam cycle maximum temperature	430 ºC
expected conversion of ammonia	0.6			Steam cycle mass flow rate	15.2 kg/s

Figure 2 shows the dependence of thermal to electric efficiency on the endothermic and exothermic reactions temperature. As seen in Figure 2a efficiency increases linearly with the endothermic reaction temperature. Figure 2b shows that there exists an exothermic reaction temperature around 450 °C, independent of the endothermic reaction temperature, at which efficiency is maximum.

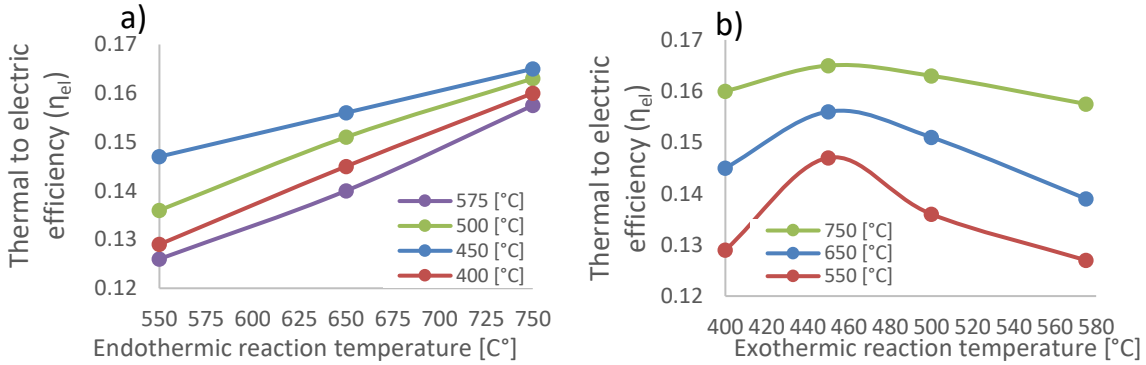

Figure 2: Thermal-to-electric efficiency as a function of a) the endothermic reaction temperature and b) the exothermic reaction temperature. The legend indicates the temperature of the opposite reactor.

As shown in Figure 2b, there is a benefit in increasing the endothermic reaction temperature whereas increasing the exothermic reaction temperature above 450 ºC is detrimental. For this base case, built upon previously reported works, thermal to electric efficiencies lower than 17 % are achieved. Other results inferred from the base case simulation are:

- There is a strong exergy loss in the heat exchanger HX-A, where a stream at 360 °C is produced by using a stream at 650 °C. The high temperature sensible heat of the effluent gases from the endothermic reactor can be used to feed a steam cycle.
- Increasing the synthesis pressure (at constant dissociation reaction pressure) can enhance the system efficiency since the compression work may be reduced. The separation process is more effective, and the heat wasted for the separation process tends to decrease with pressure.
- An isobaric system between the endothermic and exothermic reactors working at 250 bar (Luzzi et al., 1999) could improve notably the overall cycle performance.

3. System optimization

In this section a novel CSP-AL integration scheme is proposed and modelled from the previous remarks. A Pinch-Analysis (Klemeš, 2013) of the process is carried out to improve the process integration.

3.1 Pinch-Analysis

Figure 3 illustrates the pinch-analysis graphical method on the base system. A total 11.4 MW power for heating is required and the cooling power needed is 10.8 MW. The latter is referred to the heat wasted by the separator to accomplish phase separation of the products. The pinch point temperature has been detected at 98 °C, with a minimum temperature approach of 20 °C. The pinch point for hot streams occurs at 108 °C and for cold streams it takes place at 88 °C. Figure 3 has been obtained by considering only the internal streams of the systems, by excluding the power cycles from the calculations.

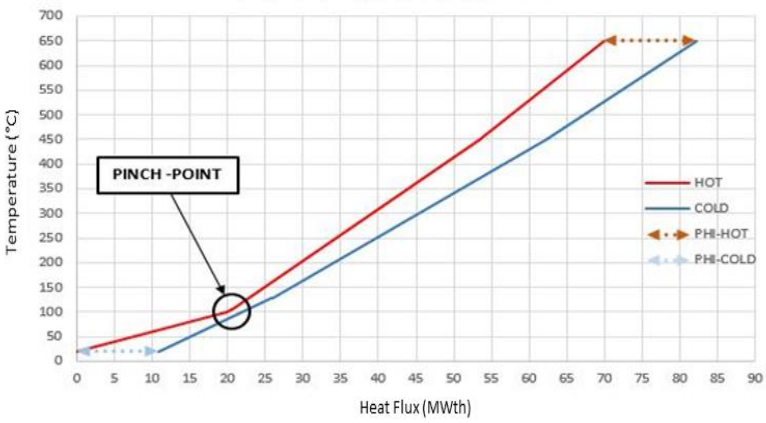

Figure 3: Hot and cold composite curves of the system internal streams, including heating and cooling requirements and pinch point temperature. Curves are based on approximated stream properties.

3.2 Heat exchangers integration

Heat exchangers integration analysis has been performed under the following constraints and assumptions: i) the heaters can be coupled only at the stream entering the endothermic and exothermic reactors; ii) the endothermic and exothermic sides are considered as independent subsystems to guarantee nominal operation in the exothermic side in the absence of solar irradiation; iii) heat exchangers characterized by low heat duty (i.e. <1 MW) are not considered; iv) data regarding thermodynamic properties of the streams have been calculated as the mean value in the temperature range of application. Figure 4 shows both the endothermic and exothermic sides heat exchangers net. In order to improve the electrical efficiency of the whole plant, the sensible heat of the stream “1.a” is used to produce superheated at 630ºC for power production. To simplify representation and to avoid including the power cycle in the analysis, the heat exchanger “PWW-3” comprises all the heat delivered from the gas exiting the dissociation reactor (stream “1”) to the power cycle. It includes pre-heater and steam generator, and super-heater for the steam cycle located in the endothermic side.

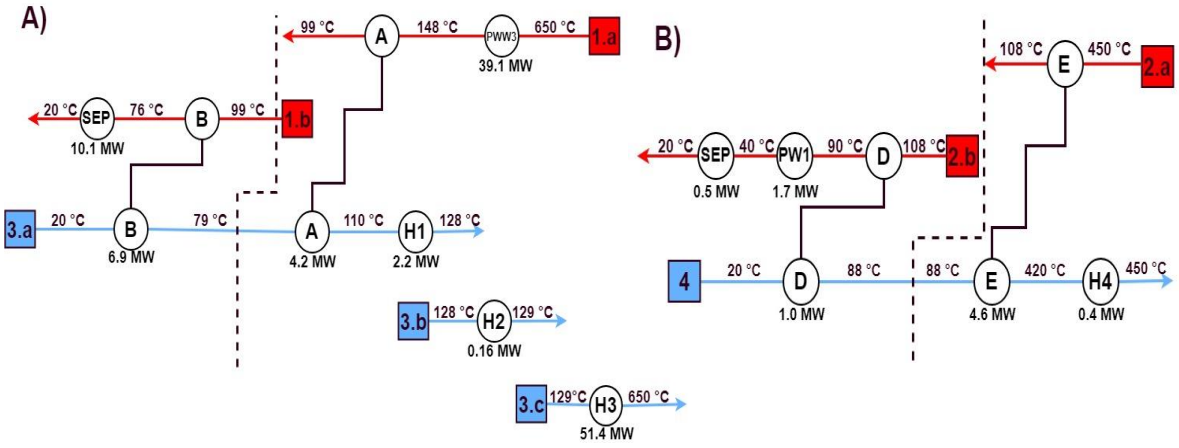

Figure 4: a) Endothermic side heat exchanger net modelled via data obtained by pinch analysis. b) Exothermic side heat exchanger net modelled via data obtained by pinch analysis.

For practical reasons, only one steam cycle will be used and the values of efficiency provided are still valid. Heaters network H1”,”H2”, “H3”, which represent the solar reactor, gives the energy needed to heat up the ammonia (stream “3”) to the reactor temperature according to the target established by Figure 3. By subtracting the “PWW-3” heat duty to the heat provided from the heaters, it is possible to match the hot requirement of the system, shown in Figure 3. The rest of solar heat provided up to 100 MWt is used to carry out the reaction. By selecting 148°C as outlet temperature leaving “PWW-3” allows a higher flexibility in the plant and ensures that, even if the mass flow rates or species concentration of any stream change, the minimum temperature approach is maintained. The heat exchanger HX-A is set to assure that no liquid fraction evolves in the outlet condition. The heat exchanged in HX-B, on the other hand, is the maximum allowed since the minimum temperature

approach is met. On the other hand, this scheme does not allow the evaporation of stream “3” (ammonia stream entering the dissociation reaction) and the phase change occurs in the endothermic reactor, here marked as “H1”,”H2” and “H3” (note that all of them are the same heat exchanger) with the consequent reduction of heat used to carry out the dissociation. The hot stream leaving the HX “B” is sent to the separator where cooling until ambient temperature occurs. The exothermic side, as mentioned above, does not have problems linked to exergy destruction in the heat exchangers.

3.3 Optimized ammonia-looping scheme

Figure 5 shows the scheme for the AL optimized scheme after the analysis carried out in the previous section.

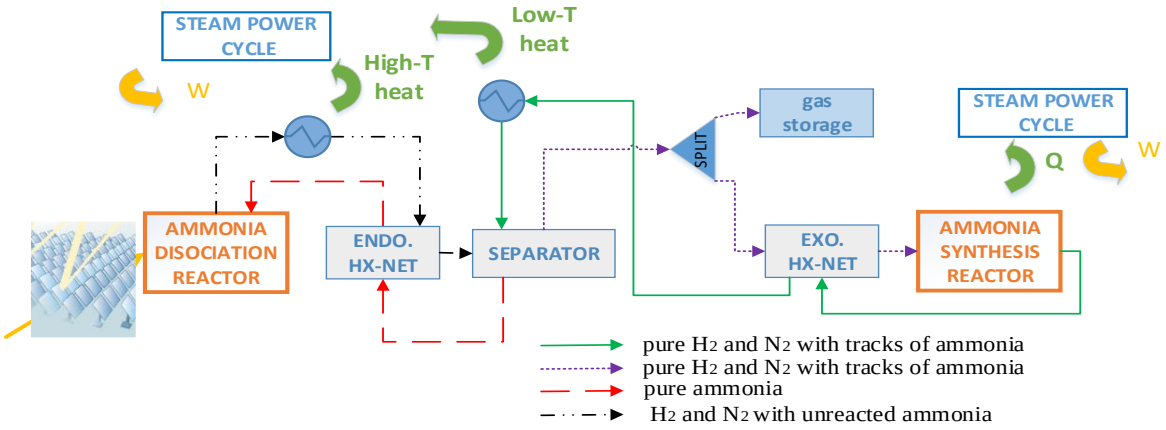

Figure 5: Flow sheet of the optimized system which comprises the integration of two steam cycles working at 630 °C and 430° C as a maximum temperature respectively. The layout has been modelled based on the pinch analysis.

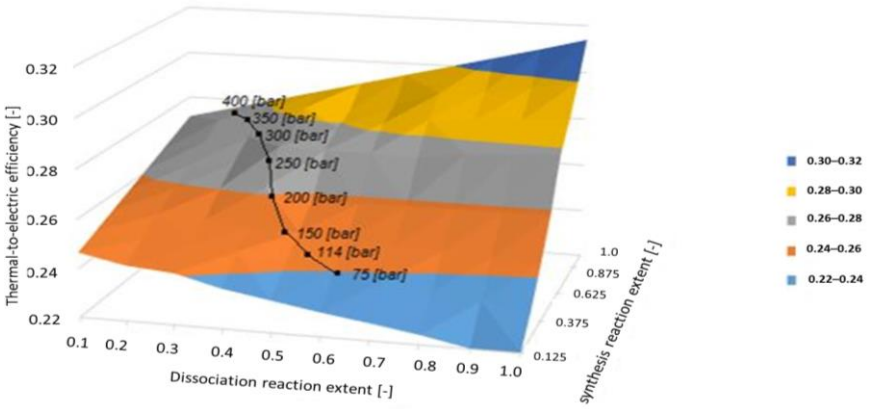

Figure 6: 3D map of thermal-to-electric efficiency as a function of reaction extent for both reactors. The pathway followed by increasing the system pressure has been marked. Split fraction=1.

This integration layout allows optimizing thermal integration by reducing the heat waste in the separation process and recovering a relevant heat fraction. As can be seen, two Rankine power cycles are considered in the scheme to differentiate the behavior of the endothermic and exothermic sides. One single steam power cycle integrating both sides could have been considered but it would have increased unnecessarily the system complexity at this conceptual stage. At other stages, and attending to practical considerations, only one power cycle would be considered to take advantage of the heat released in both endothermic and exothermic sides. Heat exchangers HX-A and HX-B, which are result of the HEN analysis, are included in the ENDO HX-NET heat exchanger network. From the optimized configuration, which is result of the HEN analysis, the split fraction between the gas storage and the EXO-HX-NET heat exchanger network is also analyzed. An increment of split fraction leads to drops of efficiency because of in the discharge phase the heat exchange PW-1 is not operative since the high-T power cycle is not working. By decreasing the split fraction, larger amount of heat is recovered during the charge phase through PW-1 and the heat progressively decreases as the split fraction increases.

Even if PW-1 is working at low temperatures and at relatively low temperature changes of the hot stream, the heat recoverable is quite high, since the condensation starts at temperatures lower than 108 °C.
Thermal to electrical efficiencies in the range of 28-30 % are achieved, whereas in the base case maximum efficiency was 17 %. Such a significant enhancement of efficiency has been obtained from the following changes: i) passing from a two-pressure system to an isobaric configuration (both reactors work at the same pressure), ii) the exothermic reaction temperature for which the thermal-to-electric efficiency optimum is 450 °C; and iii) a temperature of 650 °C has been selected for the endothermic side, since the maximum steam temperature achievable has been considered to be 630 °C for technological limitations related to materials. Figures 6 shows a sensitivity analysis on the thermal-to-electric efficiency by varying the reactor pressures and the reaction extents and where power production in the exothermic side is considered as fully independent of solar irradiation. The main parameter affecting the efficiency is represented by the system pressure. The effect of that is represented in Figure 6. For the calculation of efficiency, the following assumptions have been made: i) no thermal dispersions in the whole plant are considered, ii) charge phase lasts 8 h while discharge phase last 16 h, iii) steady state conditions are assumed, iv) the gas is stored at ambient temperature (20 °C). From Figure 6 it may be inferred that the synthesis reaction extent assumes an important role in the improvement of electrical efficiency since the steepest gradient is found along the synthesis axis.

4. Conclusions

The present work analyses the integration of an ammonia looping (AL) cycle for TCES in CSP plants. Starting from a base configuration, the process has been improved from a thermodynamic perspective. An optimized heat exchanger network has been achieved by means of a pinch analysis. Main conclusions from this work are: i) An increase of the system pressure is beneficial although an economic analysis is still needed to assess the optimal operating pressure; ii) regarding the configuration previously reported in (Luzzi et al., 1999), a similar thermal-to-electric efficiency is attained by using a heat source at lower temperature (650 ºC instead of about 850 ºC in the previous work); iii) the introduction of a high-temperature steam power cycle to recover heat from the endothermic reactor enhances the thermal-to-electric efficiency; iv) the expected thermal-to-electric efficiency for a 250 bar isobaric system is over 27 % for all values of the split fraction. Under this condition the endothermic reaction extent expected is 0.4 and 0.6 for the exothermic one; v) by increasing the endothermic reactor temperature, the efficiency is expected to be further increased; vi) for mid-temperature applications (500-650 °C), the CSP-AL integration can be judged as a potentially competitive option for TCES.

References

CSP-AL Abdiwe R., Haider M., 2017, Design of an ammonia closed-loop storage system in a csp power plant with a power tower cavity receiver, AIP Conference Proceedings, 1850, 090001.
Boisen A., Dahl S., Nørskov J.K., Christensen C.H., 2005, Why the Optimal Ammonia Synthesis Catalyst Is Not the Optimal Ammonia Decomposition Catalyst, Journal of Catalysis, 230(2), 309–312.
Dunn R., Lovegrove K, Burgess G., 2012, A review of ammonia-based thermochemical energy storage for concentrating solar power, Proceedings of the IEEE, 100, 391–400.
Klemeš J.J. (Ed), 2013, Handbook of process integration (PI): minimisation of energy and water use, waste and emissions, Woodhead Publishing Limited, Cambridge, UK.
Kreetz H., Lovegrove K., 1999, Theoretical analysis and experimental results of a 1 kw chem ammonia synthesis reactor for a solar thermochemical energy storage system. Solar Energy, 67(4–6), 287–296.
Kreetz H., Lovegrove K., Luzzi A., 2001, Maximizing thermal power output of an ammonia synthesis reactor for a solar thermochemical energy storage system, Journal of Solar Energy Engineering-Transactions of the Asme, 123(2), 75–82
Liu H., 2014, Ammonia synthesis catalyst 100 years: practice, enlightenment and challenge, Cuihua Xuebao/Chinese Journal of Catalysis, 35, 1619-1640.
Lovegrove K., 1996, High pressure ammonia dissociation experiments for solar energy transport and storage, International Journal of Energy Research, 20(11), 965–978.
Luzzi A., Lovegrove K., 1997, A solar thermochemical power plant using ammonia as an attractive option for greenhouse-gas abatement, Energy, 22, 317–325.
Luzzi, A, Lovegrove K., Filippi E., Fricker H., Schmitz-goeb M., Chandapillai M, Kaneff S., 1999, Techno-economic analysis of a 10 MW solar thermal power plant using ammonia-based thermochemical energy storage, Solar Energy, 66 (2), 91–101.
Mehos M., Turchi. C, Jorgenson J., Denholm P., Ho C., Armijo K., 2016, Advancing concentrating solar power technology, performance, and dispatchability, National Renewable Energy Laboratory, NREL/TP, Golden CO, USA, 5500-65688.
Modak, J. M., 2011, Haber process for ammonia synthesis, Resonance, 16, 1159–1167.